Symmetry and Chirality: Continuous Measures

David Avnir

The Hebrew University of Jerusalem, Israel

Hagit Zabrodsky Hel-Or

Bar-Ilan University, Ramat Gan, Israel

Paul G. Mezey

University of Saskatchewan, Saskatoon, Canada

Abbreviations

CCM = continuous chirality measure; CSM = continuous symmetry measure.

Glossary

Folding
Applying a set of inverse symmetry operations on a set of points. This procedure is one of the main steps in the folding–unfolding method for evaluating the CSM of a set of points.
Folding–unfolding method
A visual and computational procedure for evaluating the CSM of a set of points.
Fuzzy subset
A set whose elements have a range of values corresponding to the degree of membership in the set.
Fuzzy symmetry element/operator
A symmetry element/operation at a given constant fuzzy level.
Fuzzy symmetry group
A fuzzy set that has a fuzzy symmetry element at a given constant fuzzy level.
Hausdorff distance
A metric defining the distance between a point and a set or between two sets.
Symmetry deficiency measure
A measure of symmetry on crisp or fuzzy sets.
Unfolding
Applying a set of symmetry operations on a set of points. This procedure is one of the main steps in the folding–unfolding method for evaluating the CSM of a set of points.

1 INTRODUCTION: THE RATIONALE BEHIND TREATING SYMMETRY AS A CONTINUOUS STRUCTURAL PROPERTY

A traditional working tool in structural chemistry has been symmetry analysis, including that of achirality which is a special case of symmetry. Symmetry point groups and space groups have been used as reference configurations which either exist or not in the structure under study. This traditional approach fails to capture the richness of shapes and structures, both static and dynamic, which is found in the molecular and supramolecular domains. Most of these are not symmetric. At most they are approximately symmetric, either permanently or temporarily if the time-resolution of observation is sufficiently narrow.

Let us mention some very basic problems to illustrate this point. Consider two ethylene molecules approaching each other for a $[2 + 2]$ reaction. The answer to the question of whether that reaction is allowed thermally or photochemically, or whether a suprafacial or antarafacial process will take place, or whether the reaction will take place at all, is very much dependent on the symmetry of alignment of the two reacting molecules or moieties. The extremes are D_{2h} for a parallel approach and C_2 for an orthogonal approach, and it has been predicted successfully that the former is needed for a suprafacial photochemical formation of cyclobutane. Most of the time, however, the two ethylenes are not in an ideal D_{2h} arrangement. This may be due to an intramolecular frozen conformation of the two double bonds, to non-symmetric sterical hindrance caused by substituents on the double bond, and to the dynamical nature of the system (rotations and translations, especially in viscous media).

Another example is the vibrating water molecule. This is a C_{2v} molecule and its v_1 and v_2 vibrational modes preserve this symmetry. But the v_3 vibrational mode distorts the C_{2v} symmetry and again, a legitimate question is by how much does the molecule deviate from C_{2v} after 1% of one cycle, after 10% of it and so forth. Yet another example is the well-known phenomenon of removal of the degeneracy of energy levels of a chemical species whenever it is contained in an environment of symmetry other than its own (a certain arrangement of ligands or a certain packing in the crystal). The degree of removal of degeneracy is directly linked to the 'decrease' in the symmetry of the environment, compared to the isolated chemical species. Traditionally, this problem is treated in terms of jumps in the symmetry point group. For instance, the splitting of the degenerate p orbitals increases from $a_{2u} + e_u$ in a D_{4h} environment to $a_1 + b_1 + b_2$ in a C_{2v} environment.

Still another example is the concept of allowed and forbidden electronic transitions. The very weak ($\varepsilon_{\max} = 200$) forbidden $\pi \rightarrow \pi^*$ transition to the lowest lying singlet in benzene ($A_g^1 \rightarrow B_{2u}^1$), a D_{6h} symmetry molecule, changes in toluene (a molecule with a distinctly different point group, C_{2v}) only to $\varepsilon_{\max} = 225$. The discrepancy between the major symmetry change and the small effect in the 'allowedness' of the transition is currently treated in terms of perturbations and 'local' symmetry.

Chirality provides similar examples. For instance, consider the fact that ethane has various levels of D_3 in its chiral D_3 rotamers, except for the eclipsed and staggered

conformers; and that 2-deuteriobutane seems less chiral than 2-bromobutane.

These are but few examples which illustrate the need for a continuous scale of symmetry. Thus symmetry can be, and, in many instances should be, treated as a continuous property, and not necessarily as a binary property which exists or does not exist.

Several solutions to this problem, especially to the measurement of chirality, have been offered in the literature, and a selected bibliography is collected for the interested reader in Ref. 1. Here we concentrate on two approaches which proved to be versatile and suitable for treating the types of problems sketched in this introduction.

2 THE CONTINUOUS SYMMETRY MEASURE APPROACH

2.1 Elements of the Approach

This continuous symmetry measure approach to the problem of non-ideal symmetry has been guided by three principles:

1. Non-symmetric shapes should not be treated as a perturbation of an ideal reference. Such shapes, as well as perfectly symmetric ones, should appear on a single continuous scale with no built-in hierarchy of subjective ideality.
2. Assessing symmetry should be detached from referencing to a specific shape.
3. It should be possible to evaluate the symmetry of a given configuration with respect to any symmetry group.

The proposed continuous symmetry measure (CSM) method which follows these guidelines is based on the following definition.[2] Given a shape composed of n_p points P_i ($i = 1 \ldots n_p$) and a symmetry group G, the symmetry measure $S(G)$ is a function of the minimal displacement the points P_i of the shape must undergo in order to acquire G symmetry. The CSM method identifies the points $\hat{P}_i$ of the nearest shape having the desired symmetry. Once the nearest $\hat{P}_i$ values are calculated, a continuous symmetry measure is evaluated as:

$$S'(G) = \frac{1}{n_p} \sum_{i=1}^{n_p} |P_i - \hat{P}_i|^2 \qquad (1)$$

(square values are taken so that the function is isotropic, continuous, and differentiable). Prior to evaluation, one normalizes the shape by scaling about its center so that either the maximal distance of any P_i to the center is 1 (used in the examples below), or the rms of all vertex–center distances is 1. One thus obtains the limits: $0 \leq S'(G) \leq 1$. For convenience, this scale is expanded by a factor of 100

$$S(G) = 100(S'(G)) \qquad (2)$$

Thus, if a shape has the desired symmetry, $S(G) = 0$. A shape's symmetry measure increases as the shape departs from G symmetry and it reaches a maximal value (not necessarily 100 – see Appendix D in Ref. 2b). Equations (1) and (2) are general and allow one to evaluate the symmetry measure of any shape relative to any symmetry group or element. No reference shape is assumed at the beginning of the analysis, though it is obtained as an end outcome.

2.2 The Folding–Unfolding Solution

The main computational problem is then how to find the nearest object with the desired symmetry, namely the set of $\hat{P}_i$ values. For specific cases such as the distance to mirror achirality[3] or to perfect polyhedra,[4] specific shortcut calculations have been designed. However, for the general case, an approach which proved particularly useful is based on the 'folding–unfolding' algorithm.[3,4] It is based on the very method of constructing a shape which is symmetric. As an example, we build a two dimensional (2D) D_3 shape, i.e., a planar structure with one C_3 rotational symmetry element and one reflection symmetry element σ (which is equivalent to C_2 in 3D). In 2D the rotation is about a point in the plane and the reflection is through a line in the plane. The D_3 symmetry group may be of different orientations and positions (thus the rotation can be about any given point in the plane and the reflection about a line of any orientation), but a natural choice would be to consider a D_3 symmetry group where the rotation is about the origin and the reflection is about one of the axes (the y-axis). In this case, the D_3 symmetry group is of order 6 with the following elements or operations (Figure 1a):

- $g_1 = E =$ the identity
- $g_2 = \sigma =$ reflection about the y-axis
- $g_3 = C_3 =$ rotation about the origin by $2\pi/3$ radians

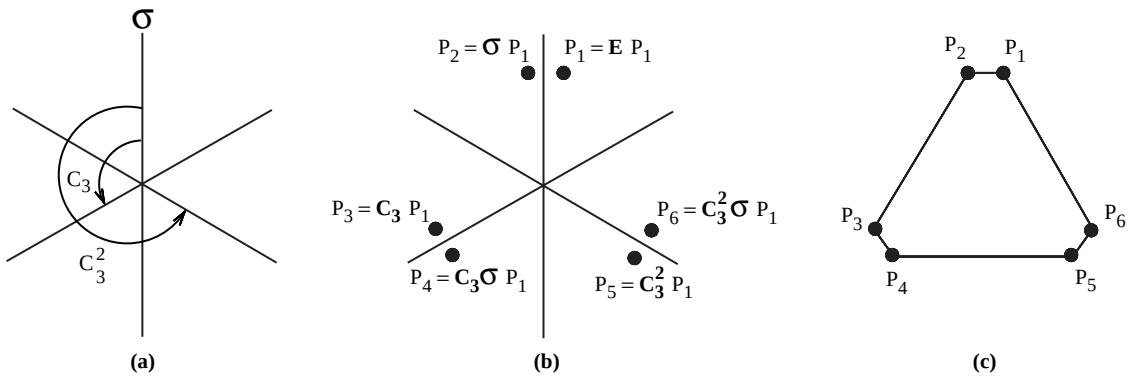

Figure 1 Creating a D_3 symmetric hexagon: (a) the D_3 symmetry group has six elements (see text); (b) applying the six group elements on the point P_1; (c) a D_3 symmetric hexagon of six points is obtained

- $g_4 = C_3\sigma$ $(= \sigma C_3^{-2})$ = rotation by $4\pi/3$ followed by reflection
- $g_5 = C_3^2$ $(= C_3^{-1})$ = rotation about the origin by $4\pi/3$ radians
- $g_6 = C_3^2\sigma$ $(= \sigma C_3)$ = rotation by $2\pi/3$ followed by reflection.

Given an arbitrary point, P_1, in an xy plane, where σ is the y-axis and C_3 rotates about the origin, a 2D D_3 symmetric arrangement of points is obtained by applying the six g_i operations, for instance, as follows (Figure 1b):

1. rotate P_1 by $2\pi/3$ radians: P_3 is obtained
2. rotate P_1 by $4\pi/3$ radians: P_5 is obtained
3. reflect P_1, P_3, P_5 about the y-axis: P_2, P_6, P_4 are obtained, respectively; a D_3 symmetric collection of six points is constructed (Figure 1c).

Such a structure can be obtained by many other orderings of the operations and many other orientations and positionings of the symmetry group. However, when connected objects, such as molecules, are of interest (in our case a hexagon) it is more natural to select that sequence of operations which follows the desired connectivity. In our D_3 example, we built the hexagon from P_1 by following the order of operations as given above which conserves the order along the hexagon boundary, i.e., $g_1 \rightarrow g_6$ (Figure 1c).

We call the procedure of obtaining a symmetric shape by applying a set of operations g_i on a point unfolding (in our example, a D_3 object is unfolded from P_1). One is usually interested in unfolding that follows a given connectivity (although the tool we develop here is applicable to disconnected assemblies as well). The inverse procedure of unfolding is folding: points $P_1, \ldots, P_6$ are folded onto P_1 by applying the inverse operations g_i^{-1}. All points coalesce onto a single point, P_1. Note, however, that if points $P_1, \ldots, P_6$ are not perfectly D_3 symmetric the folding results in a cluster of points rather than a single point. The folding–unfolding procedure is the very basis of our method for evaluating CSM values with respect to symmetry groups; the idea being to minimize the cluster spread.

In general, one can try to measure various shapes with respect to various symmetry groups. Let us explain the folding–unfolding method using the basic case where the number of points (n_p) equals the number of elements in the symmetry group (n_g) and the connectivity is cyclic. Specifically, we shall determine here how much (2D) D_3 symmetry exists in the distorted hexagon shown in Figure 2(a). The folding–unfolding method is performed as follows.

1. Determine the centroid of the object (hexagon in our case). Translate the object so that its centroid coincides with the origin and scale the object so that the maximal distance from the origin to any of the vertices is 1 (Figure 2a).
2. Translate the symmetry group so that all operations are about the origin (i.e., all rotations are about the origin and all reflection lines or planes pass through the origin).
3. Select an ordering of the n_g operations of the desired symmetry group that follows the connectivity of the P_i vertices. In our case, two orderings are possible: $g_1 \ldots g_6$ as listed above, and the reverse, $g_6 \ldots g_1$. We proceed with the first and return to the second in step 8.
4. Fold the vertices $P_1 \ldots P_6$ by applying the symmetry operation g_i^{-1} to each P_i. A cluster of folded points $\tilde{P}_1 \ldots \tilde{P}_6$ is obtained (Figure 2b). (Recall that had the object been a D_3 symmetric one, all $\tilde{P}_i$ values would coincide.)
5. Average the folded points $\tilde{P}_i$, obtaining the average point $\hat{P}_1$ (Figure 2c):

$$\hat{P}_1 = \frac{1}{n_g}\sum_{i=1}^{n_g} g_i^{-1} P_i = \frac{1}{n_g}\sum_{i=1}^{n_g} \tilde{P}_i \tag{3}$$

6. Unfold the average point $\hat{P}_1$ by applying on it each of the g_i operations and obtaining $\hat{P}_i$:

$$\hat{P}_i = g_i \hat{P}_i \quad i = 1 \ldots n_g \tag{4}$$

   The ordering $g_1 \ldots g_6$ is followed in order to retrieve the original connectivity and ordering. A D_3 symmetric shape is obtained (Figure 2d). Note that whereas the non-symmetric object is scaled to 1 (step 1), the symmetrized nearest shape is not necessarily so.
7. Calculate $S(G)$ according to equation (2).
8. Minimize the S value by repeating the folding–unfolding procedure (steps 4–7) for all orderings and all orientations of the group elements. This step is equivalent to finding the best cluster of folded points. (In the present case, due to the cyclic connectivity, minimization is reduced to the two

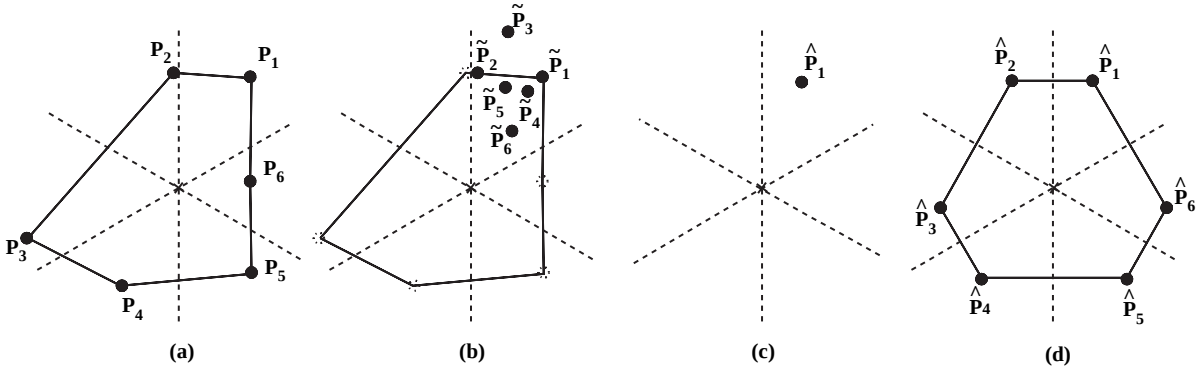

Figure 2 Measuring D_3 symmetry of a distorted hexagon using the folding–unfolding method: (a) the distorted hexagon; (b) folding the hexagon vertices in (a) – a cluster of points is obtained; (c) averaging the cluster of points in (b) – a single point is obtained; (d) unfolding the averaged point in (c) – a D_3 symmetric configuration is obtained

orderings mentioned in Step 3.) The optimal orientation is given analytically and in our case is simply 0 deg (i.e., σ is about the y-axis).[2]

Applying this procedure we find that the $S(D_3)$ value of the hexagon in Figure 2(a) is 4.89. The S value obtained by this procedure is the minimal distance to the desired symmetry group. The proof is given in Appendix A in Ref. 2b.

A common situation, however, is that the object under consideration has $n_p < n_g$ and, in particular, $n_g = l \cdot n_p$ with $l = 1, 2, 3, \ldots$. In order to deal with $n_g = l \cdot n_p$ we first explain the process of creating a G symmetric configuration of points using the unfolding process for this case. As an example, we continue with D_3 but this time with three vertices ($l = 2$, $n_p = 3$, $n_g = 6$). In general, we regard each of the n_p vertices of an $n_g = l \cdot n_p$ object as composed of l coinciding points. Thus, we regard a D_3 triangle as a hexagon in which each two vertices coincide. We construct such an object by following the general unfolding procedure with one change: the point P_1, from which the shape is unfolded, is not in a general position but is selected on a symmetry element, σ in our case (Figure 3a). It then follows that the points P_1 and P_2 coincide; therefore P_3 and P_4 coincide and so do P_5 and P_6 – an equilateral triangle is obtained. In general, l is the number of symmetry operations which leave P_1 in place (in our case $l = 2$: E and σ). In effect we divide the elements of group G into n_p sets of l elements each, such that each set G_i contains the elements of the group which bring P_1 to P_i. Thus G_1 is the set of elements which leaves P_1 in place, G_2 is the set of elements which, when applied, moves P_1 to P_2, etc. In our example (Figure 3b):

$$G_1 = \{g_1, g_2\} \qquad G_2 = \{g_3, g_4\} \qquad G_3 = \{g_5, g_6\} \tag{5}$$

Having detailed how a symmetric $n_g = l \cdot n_p$ shape is constructed, it is now clear how the folding–unfolding method is applied for evaluation of S values in such cases. The procedure is basically the same as detailed above, with some modifications, as follows.

1. Select an ordering (Figure 3c):
   (a) Determine l and divide G into n_p sets so that each set G_i contains l elements.
   (b) Select an ordering of the sets G_i of the symmetry group that follows the connectivity of the P_i vertices. (In our example the ordering is as mentioned above: G_1, G_2, G_3.)
2. Folding. For each vertex P_i, apply the inverse of the l elements of the set G_i, obtaining l folded points $\tilde{P}_{ij}\, j = 1 \ldots l$. Thus, in our example, g_1^{-1} and g_2^{-1} are applied to P_1 obtaining $\tilde{P}_{11}$ and $\tilde{P}_{12}$ (Figure 3d), g_3^{-1} and g_4^{-1} to P_2 obtaining $\tilde{P}_{21}$ and $\tilde{P}_{22}$ and so on.
3. Averaging. Average the n_g folded points. The average point $\hat{P}_1$ will always lie, in the present case, on one or more symmetry axes or planes such that applying any element of G_1 will leave it in place. In our case the averaged point, $\hat{P}_1$, must rest on the reflection line (Figure 3e). To understand this, notice that the six group

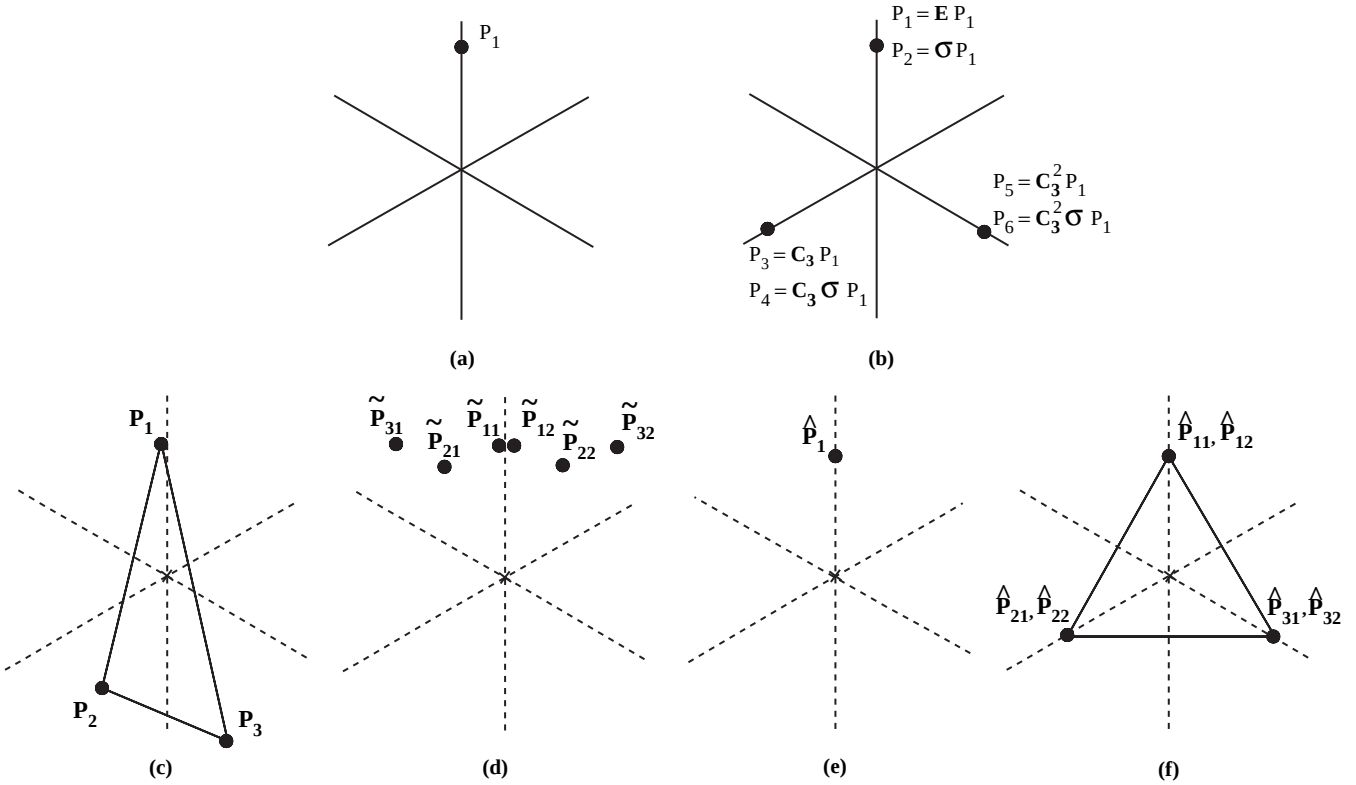

Figure 3 Creating a D_3 symmetric configuration of three points: (a) a single point P_1 is chosen on a symmetry axis; (b) unfolding P_1, one obtains three pairs of coinciding points having D_3 symmetry. Measuring D_3 symmetry of a distorted triangle: (c) the original triangle; (d) folding the points in (c) – a cluster of points is obtained; (e) averaging the cluster of points in (d) – a single point located on a symmetry axis is obtained; (f) unfolding the averaged point in (e) – a D_3 symmetric triangle is obtained

elements can be paired, i.e., E, C_3, C_3^2 and their reflections σE, σC_3, σC_3^2. On each point P_i we applied a single pair so that the obtained points P_{i1} and P_{i2} are related by σ, i.e., they are reflection of each other, and their average lies on the reflection line.

4. Unfolding. Following the unfolding step as described for the basic case we notice that since $\hat{P}_1$ remains in place under the application of elements in G_1, the unfolded points will align in n_p sets of l points each. Thus in order to obtain n_p G-symmetric points, it suffices to unfold $\hat{P}_1$ by applying a single element from each set G_i. In our case $\hat{P}_1$ unfolds into three pairs of coinciding points: $\{\hat{P}_{11}, \hat{P}_{12}\}$, $\{\hat{P}_{21}, \hat{P}_{22}\}$, $\{\hat{P}_{31}, \hat{P}_{32}\}$. By applying, for instance, only g_1, g_3, and g_5, $\hat{P}_1$, $\hat{P}_2$, and $\hat{P}_3$ are obtained (Figure 3f).

We return now to the opening question: given any number of vertices, i.e., a general non-symmetric polygon or polyhedron, what is its symmetry measure with respect to any symmetry group, subgroup, or class? The generalized approach is to divide the given points into n_s sets and to apply the folding–unfolding method separately on each set, while evaluating the S value over all the given points. For example, in the case where n_p is a multiple of n_g (i.e., $n_p = k \cdot n_g$) one divides the points into $n_s = k$ sets of n_g points each. On each set one performs the folding–unfolding method as described above. The general case, however, will typically require the division of the n_p vertices into $n_s > l$ subsets, not necessarily of equal size, but with (possibly different) l integer values for each of these sets. Once the division is made, each of the n_s subsets is symmetrized with respect to the desired symmetry group either according to the $n_g = n_p$ procedure or according to the $n_g = l \cdot n_p$ procedure. Since each of the subsets is symmetrized with respect to the same symmetry group, one obtains a symmetrization of the full set of points. Division into subsets can be performed in various ways, but in order to preserve the cyclic connectivity of the original structure (branched connectivities are treated below), the subsets must be interlaced. For details, see Ref. 2.

Finally, we comment on the case where the connectivity constrains the division into sets so that no possible division exists. For example, a cyclic connected configuration of six points cannot be divided into sets having a divisor of five points (for measuring C_5 symmetry). To overcome these specific cases one may physically duplicate or eliminate one or more of the given points. Though this has no physical or chemical interpretation, it does give a geometric solution. Thus in order to measure a triangle with respect to C_4 symmetry one duplicates one of its vertices. The symmetrized object will be with four vertices.

2.3 A 3D Example: The Non-symmetric Tetrahedron

The extension to 3D follows similar lines, and will briefly be illustrated here for the tetrahedron. T_d symmetry includes the following symmetry elements (Figure 4):

- four C_3 axes passing through the origin and through each of the four vertices (Figure 4a)
- three C_2 axes passing through the origin, each bisecting a pair of opposite edges (Figure 4b)
- six reflection planes, each containing one of the edges and bisecting the opposite edge. For our purpose only one of these reflections (σ) suffices (Figure 4c).

The 24 elements of the T_d symmetry group are thus E (the identity), four C_3 rotations (denoted $C_3(1) \dots C_3(4)$) and four C_3^2 rotations (denoted $C_3^2(1) \dots C_3^2(4)$), three C_2 rotations (denoted $C_2(12)$, $C_2(23)$, $C_2(31)$), and all the elements obtained by multiplying these elements by σ. As in the D_3 hexagon case discussed in Section 2, here too, taking an arbitrary point and applying the 24 elements (in any order) will produce a T_d symmetric 24-polyhedron. Thus, given 24 points in 3D space we can evaluate the T_d symmetry following the algorithms in Section 2. In 3D, minimization over all orientations of the symmetry group is not analytic and an iterative process is used. In most structural analyses, however, the 24-element T_d symmetry group is applied on four vertices in 3D, i.e., on the vertices of a (possibly) non-symmetric tetrahedron. This case is analogous to the case described above for D_3 symmetry of three points. Here one has $n_g = 24$, $n_p = 4$, and $l = 6$. Thus, in order to obtain a T_d symmetric set of four points (four coinciding clusters of six points) from a single point P_1, it must be positioned so that six symmetry elements of the T_d symmetry group leave it in place. Such a point lies on a C_3 axis and on a σ plane (for example, point 1 in Figure 4a). The six elements of the group that leave P_1 in place are E, C_3, and $C_3^2 (= C_3^{-1})$ and the three compositions σE, σC_3, and σC_3^2. When one applies the rest of the elements on P_1 one finds that the four sets of elements are:

$$
\begin{aligned}
G_1 &= \{E, C_3(1), C_3^2(1), \sigma, \sigma C_3(1), \sigma C_3^2(1)\} \\
G_2 &= \{C_3(3), C_3^2(4), \sigma C_3^2(2), \sigma C_3(4), C_2(12), \sigma C_2(31)\} \\
G_3 &= \{C_3^2(2), C_3(4), \sigma C_3(3), \sigma C_3^2(4), C_2(31), \sigma C_2(12)\} \\
G_4 &= \{C_3(2), C_3^2(3), \sigma C_3(2), \sigma C_3^2(3), C_2(23), \sigma C_2(23)\} \qquad (6)
\end{aligned}
$$

Thus unfolding P_1 with any one of the elements in G_2 will form P_2, with any of the elements in G_3 will form P_3, etc., creating a symmetric tetrahedron. Again, as in the previous cases, we use the construction of a symmetric shape as a guideline for the folding–unfolding procedure for evaluating the T_d symmetry of any four vertices, as follows.

Figure 4(d) shows a distorted tetrahedron. Its centroid coincides with the origin and the maximal distance to a vertex is scaled to 1. The four vertices are denoted $P_1 \dots P_4$, and a certain order of the sets G_i is selected, say $G_1 \dots G_4$, with a certain orientation of the T_d symmetry group. Each P_i is then folded by applying the six elements of the group G_i, forming a cluster of 24 points (Figure 4e). These are averaged (Figure 4f) and unfolded by selecting one element from each G_i set. For example, applying the group elements E, $C_3(3)$, $C_3^2(2)$, $C_3(2)$ to $\hat{P}_1$ we obtain, respectively, points $\hat{P}_1$, $\hat{P}_2$, $\hat{P}_3$, $\hat{P}_4$ (Figure 4g). S is then calculated from equation (2) and minimized over the two G_i orderings: G_1, G_2, G_3, G_4 and G_1, G_2, G_4, G_3 (the reason for needing only two orderings for this minimization is described in Appendix B in Ref. 2). For each of the two orderings, one minimizes S over all orientations of the symmetry group. Most tetrahedral structures of relevance in chemistry include a central atom. For treatment of this case, see Section 3.3 in Ref. 2.

In the above example we divided the points into subsets of n_g points each. However, one may divide the points into

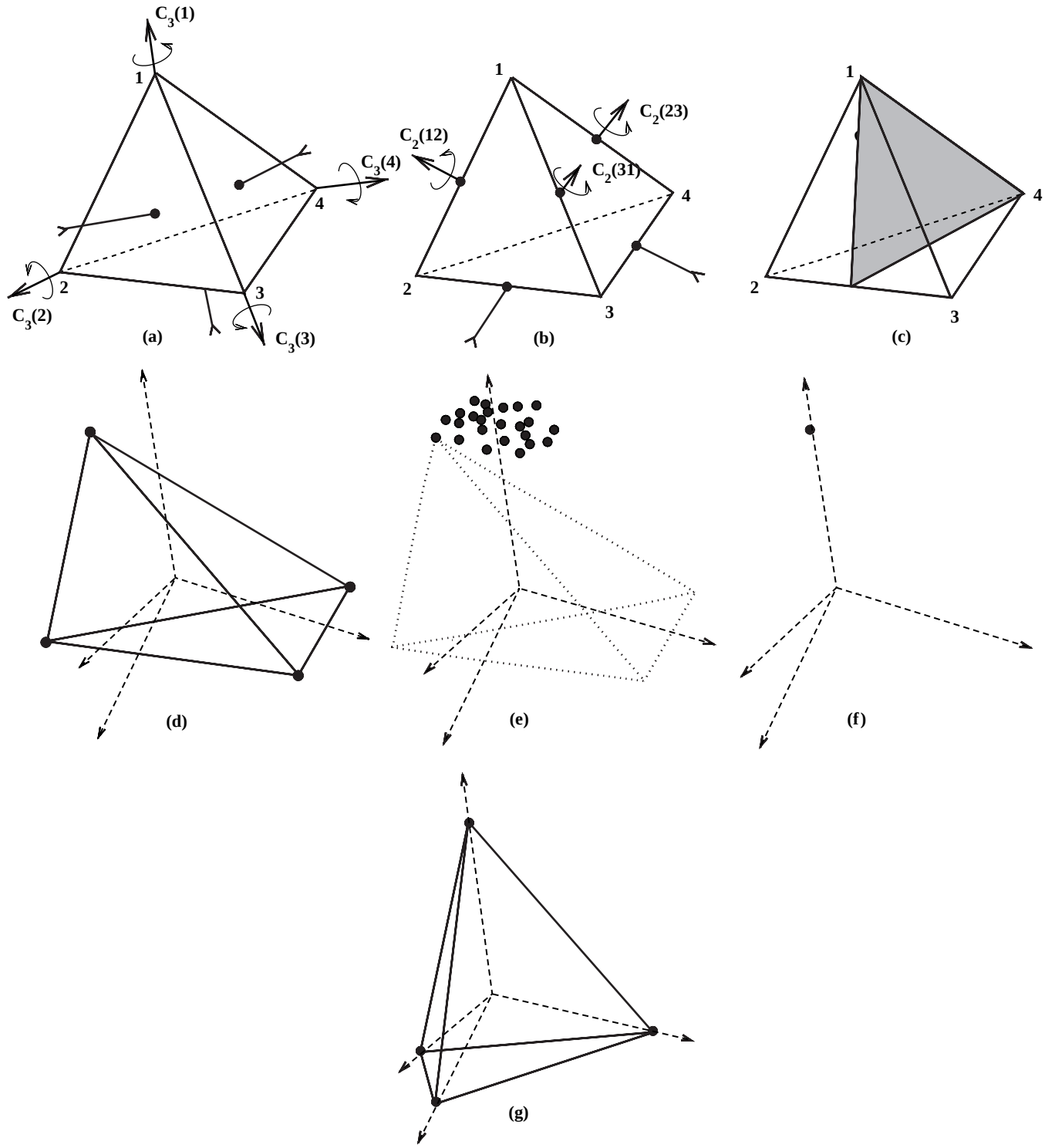

Figure 4 The symmetry elements of the T_d symmetry group include: (a) four C_3 axes, each passing through the origin and a vertex; (b) three C_2 axes, each passing through the origin, and bisecting a pair of opposite edges; (c) six reflection planes, each containing one of the edges and bisecting the opposite edge. A single plane (σ) is shown. Measuring T_d symmetry of a distorted tetrahedron: (d) the distorted tetrahedron; (e) folding the tetrahedron in (d) – a cluster of 24 points is obtained; (f) averaging the cluster of points in (e); (g) unfolding the averaged point in (f) – a T_d symmetric tetrahedron is obtained

sets having less than n_g points; specifically, into sets having a number of points which is a divisor of n_g. In this case we apply on each set the folding–unfolding method as described above for the case $n_g = l \cdot n_p$. Extending this idea further, we need not divide the points into sets of equal size. For example, let us evaluate the $S(C_{3v})$ of the tetrahedron in Figure 4(d). The C_{3v} symmetry group has $n_g = 6$ elements: E, C_3, C_3^2, and all the multiplications of these elements by σ. In order to evaluate the C_{3v} symmetry of the four points one divides them into two sets; one having three points (P_2, P_3, P_4) and one having one

point (P_1). For the first set one has $n_p = 3$ and $l = 2$ and in the second set one has $n_p = 1$ and $l = 6$. The folding–unfolding is applied as in the $n_g = l \cdot n_p$ case. One obtains two sets, each being C_{3v} symmetric, the first set consisting of three points each on a reflection plane, and the second set consisting of a single point located on the rotation axis and on the reflection planes. After minimization one obtains $S(C_{3v}) = 14.49$.

2.4 The Measurement of Achirality: The Continuous Chirality Measure (CCM) Approach

An important extension and application of the CSM approach is that S serves also as a continuous measure of chirality.[3] Since chirality is defined as a lack of certain symmetries (the improper elements), and since the CSM method allows one to evaluate how much of any of these symmetries is lacking in a given chiral configuration, one has to screen over all G_{achiral} values to find the one that provides the minimal distance to achirality. For a given set of structures, the one with the largest $S(G_{\text{achiral}})$ value is the most distant from having an improper symmetry element, and hence the most chiral; and vice versa: as $S(G_{\text{achiral}})$ approaches zero, the structure under study is minimally or negligibly chiral. In practice, since the minimal requirement for an object to be achiral is that it possesses a reflection mirror ($\sigma \equiv S_1$), an inversion center ($i \equiv S_2$) or higher order improper rotation axes S_{2n}, one has to screen S over the symmetry groups having these elements. In the majority of cases, one finds that the continuous chirality measure is simply $S(\sigma)$, i.e., the distance of a chiral object from having a reflection mirror.

The practice follows the same rationale detailed in the previous sections. Suppose we wish to construct a configuration which is symmetric with respect to the mirror symmetry group $\{E, \sigma\}$ from a given point, P_1, and a given reflection axis σ, as shown in Figure 5(a). Unless the point is on the reflection axis, the minimal number of points needed to obtain a configuration having the required symmetry is two (the number of elements in the symmetry group). Let us therefore treat the given point as a coinciding cluster of two points P_1 and P_2 (Figure 5a). To obtain a σ symmetric configuration we unfold the cluster by applying E on P_1 (being the identity element, E leaves P_1 in place, i.e., $\tilde{P}_1 = P_1$) and by applying σ on P_2 obtaining the reflected point $\tilde{P}_2$ (Figure 5b). A mirror symmetric configuration has been unfolded from the given point. The symmetric points can undergo a reversed procedure, and can be folded into a cluster of two coinciding points $\{P_1, P_2\}$. This is achieved by applying the inverse operation σ^{-1} on $\tilde{P}_2$ and E^{-1} on $\tilde{P}_1$. Notice that, whereas folding of two mirror symmetric points results in a coinciding pair of points, the folding of two non-symmetric points (Figure 5c) results in a non-coinciding cluster (Figure 5d). If the mirror axis is not predetermined, then the minimization of this distance through the search of an optimal mirror alignment is the key step in the evaluation of the minimal $S(\sigma)$. Once this minimum is found, the coordinates of the folded points are averaged obtaining the coordinates of a single average point $\hat{P}_1$ (Figure 5e), and the average point is then unfolded into a σ symmetric configuration (Figure 5f).

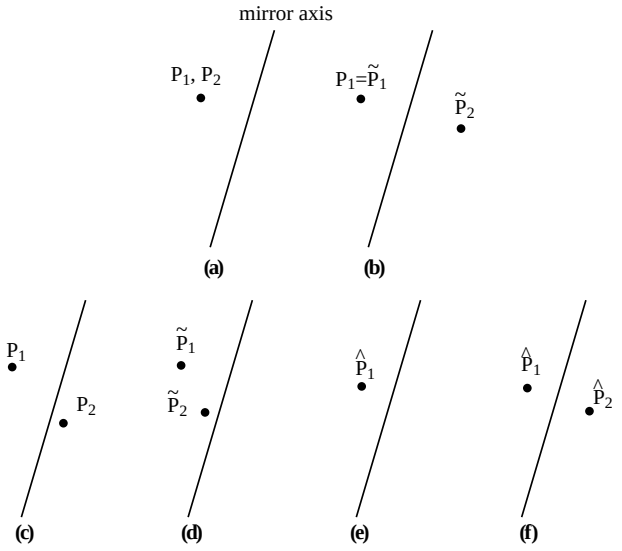

Figure 5 Top: unfolding and folding of a pair of points: (a) given a single point, one treats it as a coinciding cluster of two points P_1 and P_2; (b) unfolding the pair of points by applying the identity transformation to P_1 and reflecting P_2 across the mirror plane, a mirror symmetric pair of points, $\tilde{P}_1$ and $\tilde{P}_2$, is obtained. Bottom: treating a non-mirror symmetric pair of points, (c): (d) folding the pair of points shown in (c) results in a noncoinciding cluster of two points, $\tilde{P}_1$ and $\tilde{P}_2$; (e) the noncoinciding cluster is averaged to $\hat{P}_1$; (f) the averaged point in (e) is unfolded to a mirror symmetric pair $\hat{P}_1$ and $\hat{P}_2$

An alternative method to the folding–unfolding methodology is possible, and the problem can be reformulated so that only the folded points are considered.[3] In general, the structures we deal with are not necessarily cyclically connected as in our previous examples, but may be graph-like connected. In these cases the ordering of the operations of the group is restricted by the connectivity of the points in the original configuration, i.e., to the *topology* of the configuration.[3]

Finally we comment on chirality which is due to the lack of improper elements of symmetry other than reflection. We recall that a set of points is achiral if it has any S_n symmetry. However, for odd n, S_n is equivalent to C_{nh} and therefore includes S_1. Thus the CCM of a structure is found by finding the closest structure having S_1 or S_{2n} symmetry. The above described procedure for $S_1 \equiv \sigma$ can be straightforwardly extended to find the closest S_{2n}-symmetric configuration for any n.[3]

2.5 Demonstrated Applications of the CSM and CCM Approaches

2.5.1 Continuous Symmetry Analysis of Hyperpolarizabilities

A direct relation between the first hyperpolarizability, β, of noncentrosymmetric molecular structures and the centrosymmetricity content, $S(i)$, of such structures was shown for the first time in Ref. 5. For a series of systematic, in-plane distortions (stretch, pull, shift, and squish deformations) of the model non-linear optics chromophore benzene, a monotonic relationship between calculated values of β and $S(i)$ was found. The result suggests that the dominant variation in the hyperpolarizability for these structures arises from the change in oscillator strength.

2.5.2 Symmetry as a Process Coordinate

An important application of the continuous symmetry approach is as a process coordinate. This concept was

demonstrated and applied in a study of the dynamic interconversion between the chiral enantiomers of the water trimer,[6] one of the most intensively studied small clusters. In particular, the chirality content along several reaction pathways leading to enantiomerization, automerization, and isomerization was measured and analyzed. It was found that the interconversions occur along routes which are chiral in all their points. A favored mechanism, known as the flip mechanism, was found to be such that the chirality content is kept almost constant throughout the whole enantiomerization pathway. The non-handed structure, namely the chiral structure on that pathway for which left-handedness/right-handedness cannot be assigned under the convention used for it, was identified and recognized to be in the vicinity of the transition state of the enantiomerization. A consequence of the quantitative structural approach to chirality is the ability to identify isochiral structures, namely such that have the same degree of chirality.

2.5.3 *Analysis of the Statistical Interpretation of Symmetry and Chirality of Large Random Objects*

The structural chirality of large, random supramolecular structures, spiral diffusion-limited aggregates, was analyzed by the CCM approach. It was found[7] that classical definitions and terminologies of chirality are too restrictive for the description of such complex objects. A refined methodology and a conceptual vocabulary were developed, along with a generalized definition of chirality which takes care of supramolecular structures. The statistical significance of symmetry and chirality were defined, and applied on many examples.

2.5.4 *The Use of the Symmetry Measure as an Order Parameter*

The use of the CSM as a mathematical tool to quantify order was demonstrated in a study of the extent of cluster symmetry as a function of temperature.[8] The continuous variation of symmetry as a function of temperature was employed as a structural criterion for the follow up of melting in clusters of $(\text{ortho-}D_2)_{13}$. Thermal distribution of configurations for this cluster was obtained using the path integral Monte Carlo technique. The CSM selected to follow the structural changes of these nearly icosahedral structures was the degree of the centrosymmetricity. It was found to have better numerical properties in comparison with the standardly used rms fluctuations in the intermolecular distance, commonly applied as a criterion of cluster melting. The problem with the standardly used order parameter (d) is that on the one hand it is expected to increase significantly at a temperature at which the atoms in the cluster start exchanging places; and on the other hand one finds that the longer the simulation is, the lower is the temperature at which such exchange is obtained. The symmetry measure parameter ($S(i)$, in this case) does not suffer from that problem. Another conceptual problem with d is its definition, which assumes distinguishability between molecules. Distance between molecule n and n' is not a measurable quantity in a system of N identical molecules; however, the definition of d employs distances between labeled pairs of molecules. This problem is absent in the case of the $S(i)$ parameter as well, because it is defined uniquely for a given configuration of particles, and does not rely on particle labeling. Moreover, sampling the range of deviations of cluster configurations from perfect symmetry with respect to a given symmetry operation converges quite fast since one examines a range of typical behaviors rather than trying to sample some rare event.

2.5.5 *Continuous Chirality and Symmetry for QSAR and Drug Design*

We regard as one the most significant results of the CSM approach the observation that symmetry and chirality can be used as a predictive structural parameter for biochemical quantitative structure–activity relationship (QSAR) studies.[9] An example is the analysis of the correlation between the chirality of the pharmacophores of trypsin inhibitors and their activity. The chirality which was used was the induced one on the side chain of the inhibitor within the active site. A nice, almost linear, correlation was observed between inhibition efficiency and the degree of chirality.[9]

2.5.6 *The Quantitative Evaluation of the Degree of Chirality of Macroscopic Crystals*

The CSM and CCM approaches can, of course, be used for the analysis of macroscopic structures. An example is the treatment of the chirality of the macroscopic shape of crystals as a continuous structural property, rather than as an 'either/or' property. This was demonstrated on the classical chiral crystal of ammonium sodium tartrate.[10]

2.5.7 *Symmetry of Experimental Points with Uncertain Locations*

Information obtained from any analytical instrument has a certain degree of uncertainty. In structural chemistry, the uncertainty may be in the location of the atoms, as obtained by, e.g., diffraction methods, due to all known causes (crystal imperfections, thermal motion, etc.). Thus quite often the data is given as a collection of probability distribution functions of point locations. Given points with such uncertain locations, the following questions regarding symmetry are of interest.

- What is the most probable symmetric shape represented by the data?
- What is the probability distribution of symmetry measure values for the given data?

For treatment of these points, see Refs. 3 and 4.

3 THE FUZZY SETS APPROACH TO THE MEASUREMENT OF SYMMETRY AND CHIRALITY

We now detail a second approach to the evaluation of the degree of symmetry deficiency, from a different point of view, namely the fuzzy sets approach. Fuzzy set methods[11,12] are especially suitable to reflect the Heisenberg uncertainty relation and other aspects of quantum chemistry[13–17] and computational chemistry. Symmetry in molecules relies on the concepts of distance and metric. For the approximate symmetries of fuzzy electron densities, fuzzy set methods, fuzzy distance or fuzzy metric, and fuzzy symmetry are of importance. In Section 3.3 below, we compare and generalize the two approaches.

3.1 Some Elements of Fuzzy Set Theory

For an ordinary subset Y of a set X, $X \supset Y$, an element x of X is either a member or not a member of the subset Y; hence, by definition, the membership function $\mu_Y(x)$ of elements x of X can take only two discrete values, 1 or 0. Such ordinary sets are often referred to as 'crisp sets'.

If A is a fuzzy subset of a set X, then the elements x of X may have a whole range of possible 'commitments' to this fuzzy subset A without fully belonging to it. This is expressed by the corresponding fuzzy membership function $\mu_A(x)$ that can take any value from the $I = [0, 1]$ closed unit interval, expressing the 'degree' of point x belonging to fuzzy set A.

Set operations are naturally extended to fuzzy sets, for example: the fuzzy union $A \cup B$, the result of the operation 'A or B' is a fuzzy subset D of set U, with membership function $\mu_D(u) = \max\{\mu_A(u), \mu_B(u)\}$ for every $u \in U$.

An important tool for interrelating fuzzy problems and crisp problems is the α-cut $G_A(\alpha) = \{x : \mu_A(x) = \alpha\}$ of a fuzzy subset A of a set X, defined as the crisp set of all those points x of X with membership function $\mu_A(x)$ equal to α. A set where $\mu_A(x)$ is greater than or equal to the value α is $D_A(\alpha) = \{x : \mu_A(x) \geq \alpha\}$. These two choices for α-cuts are analogous to the electron density level sets and the density domains used in the topological analysis of molecular shapes.[14]

3.2 Fuzzy Chirality and Fuzzy Symmetry Measures

For a description of differences between fuzzy electron density clouds exhibiting approximate symmetries to various degrees, some fuzzy dissimilarity measure is needed. If in an underlying set X a metric is given, for example, the Pythagorean distance within the 3D Euclidean space E^3, then the distance between a point x of X, and a subset A of X is defined as the greatest lower bound $d(x, A) = \inf_{a \in A}\{d(x, a)\}$ of distances between points a of A and point x.

Electron density contour surfaces have the mathematical property of compactness, a generalization of the properties of 'closed' and 'bounded'. The Hausdorff distance $h(A, B)$ between two (compact) subsets A and B of X is defined as the lowest upper bound $h(A, B) = \sup_{a \in A, b \in B}\{d(a, B), d(b, A)\}$ of distances between points a of A and the set B and distances between points b of B and the set A. In particular, the Hausdorff distance between two superimposed molecular contour surfaces (which are closed sets) is the minimum r value such that any point on either contour surface has at least one point of the other contour surface within a distance r.

For fuzzy electron density clouds, the fuzzy, 'commitment-weighted' Hausdorff-type metric $f(A, B) = \sup_{\alpha \in [0,1]}\{\alpha h(G_A(\alpha), G_B(\alpha))\}$ is a proper distance between fuzzy sets A and B.[17]

A similarity measure between fuzzy electron density clouds[17] A and B is defined as $s_f(A, B) = \exp(-[f(A, B)]^2)$.

A fuzzy set A is said to have the symmetry element R corresponding to the symmetry operator $\mathbf{R}$ if and only if for each point x of A and for the transformed point $\mathbf{R}x = y$ the fuzzy membership functions fulfill the condition $\mu_A(y) = \mu_A(x)$.

For approximate symmetries, the geometrical placement of a candidate symmetry element R with respect to set A is of importance. A formal center c in set A must be given as the origin of a local coordinate system in which R is specified; furthermore, direction cosines of rotation axes and normals of reflection planes with respect to local coordinate axes are needed.

A fuzzy set A has the fuzzy symmetry element $R(\beta)$ corresponding to the symmetry operation $\mathbf{R}$ at the fuzzy level β of the fuzzy Hausdorff-type similarity measure s_g if and only if the fuzzy similarity measure s_g between $\mathbf{R}A$ and A is greater than or equal to β, $s_g(\mathbf{R}A, A) \geq \beta$. In the limit $\beta = 1$, similarity becomes indistinguishability, and the fuzzy symmetry element $R(\beta)$ becomes an ordinary symmetry element corresponding to the symmetry operation $\mathbf{R}$.

A measure of the degree of symmetry aspect R for fuzzy set A according to fuzzy Hausdorff-type similarity measure s_g is the maximum fuzzy level $\beta(A, \mathbf{R}, s_g) = \sup_{\beta \in [0,1]}\{\beta : s_g(\mathbf{R}A, A) \geq \beta\}$ at which the fuzzy symmetry element $R(\beta)$ is present for the fuzzy set A.

A fuzzy symmetry operator $\mathbf{R}(s_g)$ of fuzzy symmetry element $R(\beta')$ present for fuzzy set A at the fuzzy level β' of the fuzzy Hausdorff-type similarity measure s_g is defined by its action $\mathbf{R}(s_g)A = \mathbf{M}_{A,\mathbf{R}}\mathbf{R}A$ on the fuzzy set A, where $\mathbf{R}$ is the ordinary symmetry operator corresponding to the fuzzy symmetry element $R(\beta')$. The fuzzy indistinguishability of sets A and $\mathbf{R}A$ at the fuzzy level β' is taken into account by the operator $\mathbf{M}_{A,\mathbf{R}}$ that resets the values of fuzzy membership functions.[17]

A fuzzy set A is fully specified if for the elements x of the underlying space X the pairs $(x, \mu_A(x))$ are specified. The action of operator $\mathbf{M}_{A,\mathbf{R}}$ is $\mathbf{M}_{A,\mathbf{R}}(x, \mu_{\mathbf{R}A}(x)) = (x, \mu_A(x))$ if and only if level β' fuzzy indistinguishability is implied by the presence of the fuzzy symmetry element $R(\beta)$ at the fuzzy level β'. The application of symmetry operator $\mathbf{R}$ of fuzzy symmetry element $R(\beta')$ present at the fuzzy level β' is completed by a formal recognition of the indistinguishability of set $\mathbf{R}A$ and set A at the given fuzzy level. This additional step, for which the sufficient and necessary condition is the presence of fuzzy symmetry element $R(\boldsymbol{\beta}')$ at the fuzzy level $\boldsymbol{\beta}'$, involves operator $\mathbf{M}_{A,\mathbf{R}}$ setting the membership functions of elements of the fuzzy set $\mathbf{R}A$ equal to those of fuzzy set A.

The product of fuzzy symmetry operators $\mathbf{R}(s_g)$ and $\mathbf{R}'(s_g)$ is another fuzzy symmetry operator, $\mathbf{R}''(s_g) = \mathbf{R}(s_g)\mathbf{R}'(s_g)$. If this product is applied on a fuzzy set A that has each of the corresponding three fuzzy symmetry elements $R(\beta)$, $R'(\beta)$, and $R''(\beta)$ at fuzzy level β, then $\mathbf{R}(s_g)A$, $\mathbf{R}'(s_g)A$, and $\mathbf{R}''(s_g)A$ are indistinguishable from A at fuzzy level β.

The β' fuzzy symmetry group $G(s_g, \beta')$ (that is, the fuzzy symmetry group $G(s_g, \beta')$ at fuzzy level β') applies to fuzzy set A if A has the fuzzy symmetry element $R(\beta')$ at the fuzzy level β' of the fuzzy Hausdorff similarity measure s_g for each symmetry operation $\mathbf{R}$ of the crisp symmetry group G.

The symmetry deficiency measure $\delta(A, \mathbf{R}, s_g)$ of fuzzy set A in symmetry element R according to the fuzzy Hausdorff-type similarity measure s_g is defined as $\delta(A, \mathbf{R}, s_g) = 1 - \beta(A, \mathbf{R}, s_g)$.

A fuzzy set A is an R set with respect to a family of symmetry elements, $R = \{R_1, R_2, \ldots, R_m\}$ if A has all the symmetry elements of family R.

Fuzzy set B' is a maximal R subset of fuzzy set A if $A \supset B'$, B' is an R set, and no R set B'' exists such that $B'' \supset B'$, $B' \neq B''$, and $A \supset B''$. Note that the fuzzy, maximal R subset of B' is not necessarily unique for a given fuzzy set A.

The cardinality $m(A) = \int_X \mu_A(x)\,\mathrm{d}x$ of a fuzzy set A can be regarded as the mass of fuzzy set A. For fuzzy electron density

clouds A of molecules this mass $m(A)$ can be interpreted as electronic charge.

A fuzzy set B is a maximal mass R subset of fuzzy set A if B is a fuzzy R set, $A \supset B$, and if for all maximal fuzzy R subsets B' of fuzzy set A, $m(B') \leq m(B)$. The fuzzy, maximal mass R subset B is not necessarily unique for a given fuzzy set A; however, the mass $m(B)$ is already a unique number for each fuzzy set A.

A fuzzy set C' is a minimal R superset of fuzzy set A if C' is an R set, $C' \supset A$, and if no fuzzy R set C'' exists such that $C' \supset C''$, $C' \neq C''$, and $C'' \supset A$. The fuzzy, minimal R superset C' is not necessarily unique for a given fuzzy set A.

Fuzzy set C is a minimal mass R superset of fuzzy set A if C is an R set, $C \supset A$, and if for all minimal fuzzy R supersets C' of fuzzy set A, $m(C) \leq m(C')$. A fuzzy minimal mass R superset C is not necessarily unique for a given fuzzy set A; however, the mass $m(C)$ is a unique number for each fuzzy set A. If the fuzzy set A itself is an R set then both B and C are unique and $B = C = A$.

The internal fuzzy R deficiency measure of a fuzzy set A is $\delta_{R,B}(A) = 1 - m(B)/m(A)$ where B is the maximal mass fuzzy R subset of fuzzy set A.

The external fuzzy R deficiency measure of a fuzzy set A is $\delta_{R,C}(A) = 1 - m(A)/m(C)$ where C is the minimal mass fuzzy R superset of fuzzy set A.

The fuzzy R deficiency measure $\delta_R(A) = (\delta_{R,B}(A) + \delta_{R,C}(A))/2$ of fuzzy set A is the average of the above two measures.

For any fuzzy R subset B', R superset C', maximal mass fuzzy R subset B, and minimal mass fuzzy R superset C of any fuzzy set A, the relations $m(B') \leq m(C')$ and $m(C) - m(B) \leq m(C') - m(B')$ hold.

For a chiral fuzzy object A, the largest achiral fuzzy object that fits within A, as well as the smallest achiral fuzzy object that contains A, are of special importance.

Fuzzy set B' is a maximal achiral subset of fuzzy set A if B' is achiral, $A \supset B'$, and if no achiral fuzzy set B'' exists such that $B'' \supset B'$, $B' \neq B''$, and $A \supset B''$. Note that a maximal achiral subset B' is not necessarily unique for a given fuzzy set A.

Fuzzy set B is a maximal mass achiral subset of fuzzy set A if B is achiral, $A \supset B$, and if for the fuzzy volumes of all maximal achiral subsets B' of fuzzy set A, the inequality $m(B') \leq m(B)$ applies. Note that, for a given fuzzy set A, such a maximal mass achiral subset B is not necessarily unique. Nevertheless, the fuzzy mass $m(B)$ is a unique number for each fuzzy set A.

A fuzzy set C' is a minimal achiral superset of a fuzzy set A if C' is achiral, $C' \supset A$, and if no achiral fuzzy set C'' exists such that $C' \supset C''$, $C' \neq C''$, and $C'' \supset A$. Note that a minimal achiral superset C' is not necessarily unique for a given fuzzy set A.

Fuzzy set C is a minimal mass achiral superset of fuzzy set A if fuzzy set C is achiral, $C \supset A$, and for all minimal achiral supersets C' of fuzzy set A, $m(C) \leq m(C')$. For a given fuzzy set A, a minimal mass achiral superset C is not necessarily unique. Nevertheless, the mass $m(C)$ is a unique number for each fuzzy set A. If fuzzy set A is achiral then both the minimal achiral fuzzy superset B and the minimal mass achiral fuzzy superset C are unique and $B = C = A$.

The internal fuzzy chirality measure of a fuzzy set A is defined as $\chi_B(A) = 1 - m(B)/m(A)$ where B is a maximal mass achiral subset of fuzzy set A. The measure $\chi_B(A)$ is a natural, fuzzy set extension of the measure obtained using the maximum overlap criterion between mirror images.

The external fuzzy chirality measure of a fuzzy set A is defined as $\chi_C(A) = 1 - m(A)/m(C)$ where C is a minimal mass achiral superset of fuzzy set A.

The fuzzy chirality measure $\chi(A) = (\chi_B(A) + \chi_C(A))/2$ is the average of the above two measures.

3.3 Comparisons of Symmetry Measures for Discrete Point Sets of Nuclear Arrangements and Continua of Electron Densities

The CSM described in Section 2 is a symmetry deficiency measure which is applicable to both discrete sets and to continua. For crisp continuum sets and fuzzy sets, the crisp and fuzzy versions of the Hausdorff metric provide generalizations of the CSM approach.

3.3.1 Symmetry Measures for Discrete Sets and Crisp Sets

A typical discrete set of chemical importance is a nuclear arrangement in the clamped nucleus version of the Born–Oppenheimer approximation. A single molecular isodensity contour (MIDCO) surface is a crisp continuum set. A simple generalization of the CSM approach from finite, discrete point sets to continua is provided by the crisp average of sets.

3.3.1.1 Crisp average. The crisp average A_{crav} of a family $F_A = \{A_1, A_2, \ldots, A_m\}$ of m crisp closed and bounded subsets A_i of an n-dimensional Euclidean space X is generated as follows. Each point x of a set A_i is represented by suitable hyperpolar coordinates of one radial coordinate and $n - 1$ angle coordinates, where n is the dimension of the underlying space X and the origin is attached to a specified point c of set A_i. In three dimensions, the usual polar coordinates r, ϕ, and θ can be used, with respect to the center c of each set A_i and with reference to Cartesian coordinate axes defined parallel to axes of a coordinate system of the laboratory frame.

For each set A_i, its convex hull C_i is unique. In the 3D case, for each choice of the (ϕ, θ) pair, a unique line segment $q_i(\phi, \theta)$ is specified that connects a selected reference point $c_i \in C_i$ of A_i with the unique point $y_i(\phi, \theta) \in C_i$ which is the point of polar angle coordinates (ϕ, θ) with the longest distance from center c_i, $d(c_i, y_i(\phi, \theta)) = \sup\{d(c_i, x)\colon x = x(\phi, \theta), x \in C_i\}$. Whereas along this line segment $q_i(\phi, \theta)$ some points do not necessarily belong to set A_i, nevertheless, the formal path parametrization along the line $q_i(\phi, \theta)$ varies only within set A_i and ignores any missing subsegments.

A parametrization for the formal path $q_i(u, (\phi, \theta))$ for each fixed pair (ϕ, θ) is a mapping from the unit interval $I = [0, 1]$ to the underlying space X. The image of this mapping is the line segment $q_i(\phi, \theta)$ parametrized by u, $q_i(u, (\phi, \theta))$, where $q_i(0, (\phi, \theta)) = c_i$, and $q_i(1, (\phi, \theta)) = y_i(\phi, \theta)$, and where u is proportional to the arc length, $q_i(u, (\phi, \theta))\colon I = [0, 1] \rightarrow q_i(\phi, \theta)$, $X \supset q_i(\phi, \theta)$.

A parameter $t(w, (\phi, \theta))$ is defined in terms of the membership function $\mu_{Ai}(x)$ of crisp set A_i, $t_i(w, (\phi, \theta)) = \int_{[0,w]} \mu_{Ai}(q_i(z, (\phi, \theta)))\mathrm{d}z$, where integration is for the subset $[0, w]$ of the unit interval $I = [0, 1]$. This parameter $t_i(w, (\phi, \theta))$ 'leaves out the gaps' along line $q_i(\phi, \theta)$. Scaling $t_i(w, (\phi, \theta))$ by the effective length $t_i(1, (\phi, \theta))$ of line segment $q_i(\phi, \theta)$ within set A_i, defines the function $v_i(w, (\phi, \theta)) = t_i(w, (\phi, \theta))/t_i(1, (\phi,$

$\theta)$). A possibly discontinuous path $p_i(u, (\phi, \theta))$: $I = [0, 1] \rightarrow q_i(\phi, \theta) \cap A_i, X \supset q_i(\phi, \theta) \cap A_i$ along segment $q_i(\phi, \theta)$ involves only those points of $q_i(\phi, \theta)$ which fall within set A_i, that is, $p_i(u, (\phi, \theta)) = q(v_i^{-1}(u, (\phi, \theta)))$.

Each point $x \in q_i(\phi, \theta) \cap A_i$ can be specified uniquely by a set of three polar coordinates, (u, ϕ, θ), and the serial index i of set A_i, $x = x(i, u, \phi, \theta)$. For each trio of values (u, ϕ, θ), there exists precisely one point $x(i, u, \phi, \theta)$ that must be an element of set A_i. Conversely, each point x of each set A_i can be given in the form $x = x(i, u, \phi, \theta)$, providing a unified system of parametrization for points of each set $A_1, A_2, \ldots, A_m$.

The crisp average $A_{\text{crav}}(F_A) = \cup_{u,\phi,\theta}(1/m)\Sigma_{i=1,m}x(i, u, \phi, \theta)$ of sets $A_1, A_2, \ldots, A_m$ is defined by the union of the averaged vector representations of points $x(i, u, \phi, \theta)$.

3.3.1.2 Generalization of the CSM approach from finite, discrete point sets to continua based on the crisp average of sets. For a set A, and a (possibly approximate) symmetry element R of symmetry operator $\mathbf{R}$ leaving at least one point of the convex hull C of set A invariant, take the powers $\mathbf{R}^0 = \mathbf{E}, \mathbf{R}, \mathbf{R}^2, \ldots, \mathbf{R}^{m-1}$ of the symmetry operator $\mathbf{R}$, where m is the smallest positive integer that satisfies the condition $\mathbf{R}^m = \mathbf{E}$. Partition the Euclidean space X into m segments $X_0, X_1, \ldots, X_{m-1}$, where $X = \cup_{i=0,m-1}X_i$, and $\mathbf{R}X_i = X_{(i+1)\bmod m}$. If R is a reflection plane, then $m = 2$, and the two half spaces with boundary plane the reflection plane R fulfill the conditions. If R is a C_k rotation axis or an S_k axis, then $m = k$, and each segment of the Euclidean space X can be taken as a wedge of edge the C_k or the S_k axis, and wedge angle $2\pi/k$. If R is a point of inversion i, then $m = 2$, and the two half spaces with boundary plane (x, y) fulfill the conditions. The notation P is used for the specification of the actual convention used in the positioning of R with respect to crisp continuum set A and for the partitioning $X_0, X_1, \ldots, X_{m-1}$ of the space X.

Using segments $A_0, A_1, \ldots, A_{m-1}$ of set A, $A_i = A \cap X_i$, the sets $A_0, \mathbf{R}^{m-1}A_1, \mathbf{R}^{m-2}A_2, \ldots, \mathbf{R}^{m-j}A_j, \ldots, \mathbf{R}A_{m-1}$ are generated. The sets $B_j = \mathbf{R}^{m-j}A_j$ are the various 'folded' versions of subsets A_j of set A. The folded set $A_{\text{fold}} = A_{\text{crav}}(F_A) = \cup_{u,\phi,\theta}(1/m)\Sigma_{i=0,m-1}x(i, u, \phi, \theta)$ is defined as the crisp average of these B_j sets.

The gradual 'unfolding' of this crisp average $A_{\text{crav}}(F_A)$ using various inverse powers of symmetry operator $\mathbf{R}$ leads to the sets A_{fold}, $\mathbf{R}^{1-m}A_{\text{fold}}$, $\mathbf{R}^{2-m}A_{\text{fold}}, \ldots, \mathbf{R}^{j-m}A_{\text{fold}}, \ldots, \mathbf{R}^{-1}A_{\text{fold}}$. The folded–unfolded set $A_{\text{f,uf},R,P}$ of set A according to symmetry element R and partitioning P is the union $A_{\text{f,uf},R,P} = \cup_{i=0,m-1}\mathbf{R}^{-i}A_{\text{fold}}$. The folded–unfolded set $A_{\text{f,uf},R,P}$ of set A has the exact R symmetry and is evidently an R set.

The dissimilarity of A and $A_{\text{f,uf},R,P}$ provides a symmetry deficiency measure analogous to the CSM continuous symmetry measure of discrete point sets. As a dissimilarity measure, the Hausdorff metric, or any other dissimilarity measure suitable for continua may be used. Using the extension of the CSM methodology to crisp continuum sets, the folding–unfolding approach becomes applicable for continuous molecular isodensity surfaces.

3.3.2 Symmetry Measures for Continuum Sets

A typical fuzzy continuum of chemical importance is an electron density cloud of a molecule. The fuzzy average of crisp or fuzzy subsets $F_1, F_2, \ldots$, and F_m of a set X can be interpreted as a fuzzy subset F_{fav}, defined by its fuzzy membership function $\mu_{F\text{fav}}(x) = [\Sigma_{k=1,m}\mu_{Fk}(x)]/m$. Note that the fuzzy average F_{fav} of crisp sets $F_1, F_2, \ldots$, and F_m is a crisp set if and only if $F_1 = F_2 = \cdots = F_m$, then, of course, $F_{\text{fav}} = F_1$ also holds.

Take a crisp or fuzzy subset A of the Euclidean space X, a possibly approximate symmetry element R, and the associated symmetry operator $\mathbf{R}$. A reference point $c \in X$ is chosen as a fixed point of R. Point c is taken as the origin of a local Cartesian coordinate system of axes oriented according to the usual conventions with respect to the symmetry operator $\mathbf{R}$.

If m is the smallest positive integer that satisfies the condition $\mathbf{R}^m = \mathbf{E}$ for the symmetry operator $\mathbf{R}$, then the Euclidean space X is partitioned into m segments X_i, where $X = \cup_{i=0,m-1}X_i$, and $\mathbf{R}X_i = X_{(i+1)\bmod m}$.

The segment A_i of the crisp or fuzzy set A is defined as $A_j = A \cap X_j$, and the 'folded' version of the j-th segment A_j of the crisp or fuzzy set A according to the $(m - j)$-th power $\mathbf{R}^{m-j}$ of the (possibly only approximate) symmetry operator $\mathbf{R}$ is denoted by $B_j = \mathbf{R}^{m-j}A_j$. For the family S_A of segments $A_0, A_1, A_2, \ldots, A_{m-1}$, the corresponding folded sets $B_0 = A_0$, $B_1 = \mathbf{R}^{m-1}A_1$, $B_2 = \mathbf{R}^{m-2}A_2, \ldots, B_{m-2} = \mathbf{R}^{m-j}A_j, \ldots$, and $B_{m-1} = \mathbf{R}A_{m-1}$ are generated. In terms of the fuzzy membership functions of these B_j sets the fuzzy folded set A_{ffold} is defined as the fuzzy average $S_{B\text{fav}}$ with the fuzzy membership function $\mu_{A\text{ffold}}(x) = \mu_{SB\text{fav}}(x) = [\Sigma_{k=0,m-1}\mu_{Bk}(x)]/m$. The fuzzy folded set A_{ffold} is unfolded using the appropriate inverse powers of symmetry operator $\mathbf{R}$, generating the following sets: A_{ffold}, $\mathbf{R}^{1-m}A_{\text{ffold}}$, $\mathbf{R}^{2-m}A_{\text{ffold}}, \ldots, \mathbf{R}^{j-m}A_{\text{ffold}}, \ldots, \mathbf{R}^{-1}A_{\text{ffold}}$. The folded–unfolded fuzzy set $A_{\text{ff,uf},R,P}$ of crisp or fuzzy set A with respect to symmetry element R and partitioning P is the fuzzy union $A_{\text{ff,uf},R,P} = \cup_{j=0,m-1}\mathbf{R}^{-j}A_{\text{ffold}}$. The folded–unfolded set $A_{\text{ff,uf},R,P}$ is a fuzzy R set by construction.

The fuzzy Hausdorff-type dissimilarity metric $f(A, B)$ can be applied to the pair A and $A_{\text{ff,uf},R,P}$, generating a fuzzy symmetry deficiency measure $f(A, A_{\text{ff,uf},R,P})$ analogous to the CSM of discrete point sets. This symmetry deficiency measure $f(A, A_{\text{ff,uf},R,P})$ provides a measure for the symmetry aspect R for crisp or fuzzy set A, with reference to the given positioning P of R with respect to A and to the choice of the associated partitioning of A.

The infimum $f(A, A_{\text{ff,uf},R,P}) = \inf_P\{f(A, A_{\text{ff,uf},R,P})\}$ taken over all the allowed positionings and partitionings P gives another symmetry deficiency measure. These symmetry deficiency measures are equally applicable to discrete sets, crisp continuum sets, and fuzzy sets, including nuclear distributions and fuzzy electron density distributions of molecules, molecular fragments, and functional groups.

4 OUTLOOK: APPLICATIONS BEYOND CHEMISTRY

In Section 2.5 we demonstrated applications and potential future uses of the CSM approach in chemistry. It is now in order to point out that the general foundations laid out in this article, and the versatility of the computational approach, are, in principle, applicable to the analysis of symmetry and chirality-related problems in many other domains of the natural sciences and social sciences. The following examples hint at the vastness of the new open horizons:

- symmetry determination in automated image analyses for quality control of industrial products[18]
- symmetry analysis of facial features for forensic, psychological, and artistic analyses[18]
- symmetry analysis as a quantitative measure of cultural development of early humans[19]
- chirality and symmetry analyses of random spiral aggregates such as galaxies, clouds, tornadoes, and molecular scale aggregates
- symmetry issues in medicine, as an analytical, diagnostic, and classification biomedical tool – many other structural features of living organisms are analyzable in terms of bilateral symmetry and deviations from it, and are potentially useful as indicators of pathological conditions
- symmetry analysis in evolutionary sociobiology, one of the most active issues in modern biology
- quantification of symmetry for the study of aesthetics
- symmetry analysis of information packets (stock behavior, music, process reproducibility, error occurrence, etc.).

This list is but a sketch of some of the many potential applications of the continuous symmetry methodology approach. The feasibility of the first three applications in this list have already been proven successful.[18,19]

5 RELATED ARTICLES

Cambridge Structural Database; Canonical Numbering and Constitutional Symmetry; Combinatorial Libraries: Structure–Activity Analysis; Complete Active Space Self-consistent Field (CASSCF) Second-order Perturbation Theory (CASPT2); Computer Graphics and Molecular Modeling; Drug Design; Geometry Optimization: 1; Geometry Optimization: 2; Graph Theory in Chemistry; Pericyclic Reactions: The Diels–Alder Reaction; Pharmacophore and Drug Discovery; Quantitative Structure–Activity Relationships in Drug Design; Quantitative Structure–Property Relationships (QSPR); Shape Analysis; Structural Chemistry: Application of Mathematics; Symmetry-derived Methods for Obtaining Graph Spectra; Symmetry in Chemistry; Symmetry in Hartree–Fock Theory; Topological Indices; Topological Methods in Chemical Structure and Bonding; Water Clusters; X-Ray Crystallographic Analysis and Semiempirical Computations.

6 REFERENCES

1. Bibliography of selected papers on the measurement of chirality and symmetry: (a) A. I. Kitaigorodskii, 'Organic Chemical Crystallography', Consultants Bureau, New York, 1961, Chap. 4; (b) A. Rassat, *C. R. Acad. Sci. Paris II*, 1984, **299**, 53–55; (c) G. Gilat, *Chem. Phys. Lett.*, 1985, **121**, 9–12; (d) P. G. Mezey and J. Maurani, *Mol. Phys.*, 1990, **69**, 97–113; (e) P. G. Mezey (ed.), 'New Developments in Molecular Chirality', Kluwer, Dordrecht, 1991; (f) N. Weinberg and K. Mislow, *J. Math. Chem.*, 1993, **14**, 427–450; A. B. Buda and K. Mislow, *J. Am. Chem. Soc.*, 1992, **114**, 6006–6012; (g) G. Gilat and L. S. Schulman, *Chem. Phys. Lett.*, 1985, **121**, 13–16; (h) G. Gilat, *J. Phys. A: Math. Gen.*, 1989, **22**, L545–L547; (i) A. Seri-Levy and W. G. Richards, *Tetrahedron: Asymm.*, 1993, **4**, 1917–1923; (j) E. Cavali and R. Cammi, *Comput. Chem.*, 1994, **18**, 405–411; (k) W. Kauzmann, F. B. Clough, and I. Tobias, *Tetrahedron*, 1961, **13**, 57–105; (l) E. Ruch, *Acc. Chem. Res.*, 1972, **5**, 49–56; (m) M. Raji and A. Cossé-Barbi, *C. R. Acad. Sci. Paris II*, 1997, **324**, 133–138; (n) Z. Zimpel, *J. Math. Chem.*, 1993, **14**, 451–465; (o) J. F. Donoghue, E. Golowich, and B. R. Holstein, *Phys. Rev. D.*, 1984, **30**, 587–593; (p) V. E. Kuz'min, I. B. Stel'mach, M. B. Bekker, and D. V. Pozigun, *J. Phys. Org. Chem.*, 1992, **5**, 295–298; (q) A. V. Luzanov and E. N. Babich, *Struct. Chem.*, 1992, **3**, 175–181; (r) Y. Hel-Or, S. Peleg, and D. Avnir, *Langmuir*, 1990, **6**, 1691–1695; Erratum: 1994, **10**, 1633; (s) A. Y. Meyer and W. G. Richards, *J. Comput.-Aided Mol. Design*, 1991, **5**, 427–439; (t) P. Murray-Rust, H. B. Bürgi, and J. D. Dunitz, *Acta Crystallogr., Sect. B*, 1978, **34**, 1787–1793; (u) M. A. Osipov, B. T. Pickup, and D. A. Dunmur, *Mol. Phys.*, 1995, **84**, 1193–1206; (v) D. J. Klein, *J. Math. Chem.*, 1995, **18**, 321–348; (w) H. C. Longuet-Higgins, *Mol. Phys.*, 1963, **6**, 445–460; (x) A. P. Toporova, A. A. Toporov, M. M. Ishankhodzhaeva, and N. A. Parpirev, *Russ. J. Inorg. Chem.*, 1996, **41**, 466–469; (y) B. Grunbaum, *Proc. Symp. Pure Math.: Am. Math. Soc.*, 1963, **7**, 233–270; (z) G. Marola, *IEEE Trans. Pattern Anal. Machine Intell.*, 1989, **11(1)**, 104–108; (aa) Y. Hel-Or, S. Peleg, and D. Avnir, *Comput. Vision, Graphics Image Process.*, 1991, **53(2)**, 297–302; (bb) A. I. Kitaigorodskii, 'Organic Chemical Crystallography', Consultants Bureau, New York, 1961; (cc) R. Chanvin, *J. Math. Chem.*, 1996, **19**, 147–174; (dd) G. Moreau, *J. Chem. Inf. Comput. Sci.*, 1997, **37**, 929–938.
2. (a) H. Zabrodsky, S. Peleg, and D. Avnir, *J. Am. Chem. Soc.*, 1992, **114**, 7843–7851; (b) H. Zabrodsky, S. Peleg, and D. Avnir, *J. Am. Chem. Soc.*, 1993, **115**, 8278–8289.
3. H. Zabrodsky and D. Avnir, *J. Am. Chem. Soc.*, 1995, **117**, 462–473.
4. (a) H. Zabrodsky and D. Avnir, *Adv. Mol. Struct. Res*, 1995, **1**, 1–30; (b) M. Pinsky and D. Avnir, manuscript in preparation.
5. D. Kanis, J. Wong, T. Marks, M. Ratner, H. Zabrodsky, S. Keinan, and D. Avnir, *J. Phys. Chem.*, 1995, **99**, 11061–11066.
6. Y. Pinto, H. Z. Hel-Or, and D. Avnir, *J. Chem. Soc., Faraday Trans.*, 1996, **92**, 2523–2527.
7. O. Katzenelson, H. Hel-Or, and D. Avnir, *Eur. J. Chem. A*, 1996, **2**, 174–181.
8. V. Buch, E. Greshgoren, H. Z. Hel-Or, and D. Avnir, *Chem. Phys. Lett.*, 1995, **247**, 149–153.
9. (a) D. Avnir, O. Katzenelson, S. Keinan, M. Pinsky, Y. Pinto, Y. Salomon, and H. Z. Hel-Or, in 'Concepts in Chemistry', ed. D. H. Rouvray, Research Studies Press, Somerset, 1996, Chap. 9, pp. 283–324; (b) S. Keinan and D. Avnir, 1996 **http://www.chem.ch.huji.ac.il/employee/avnir/watoc96/poster.html**
10. S. Keinan, H. Z. Hel-Or, and D. Avnir, *Enantiomer*, 1996, **1**, 351–357.
11. L. A. Zadeh, *Inf. Control*, 1965, **8**, 338–345.
12. G. J. Klir and B. Yuan, 'Fuzzy Sets and Fuzzy Logic, Theory and Applications', Prentice Hall, Upper Saddle River, NJ, 1995.
13. P. G. Mezey, 'Potential Energy Hypersurfaces', Elsevier, Amsterdam, 1987.
14. P. G. Mezey, 'Shape in Chemistry: An Introduction to Molecular Shape and Topology', VCH Publishers, New York, 1993.
15. P. G. Mezey, *Adv. Quantum Chem.*, 1996, **27**, 163–222.
16. P. G. Mezey, *Int. J. Quantum Chem.*, 1997, **63**, 39–48.
17. P. G. Mezey, in 'Fuzzy Logic in Chemistry', ed. D. H. Rouvray, Academic Press, San Diego, CA, 1997.
18. (a) H. Zabrodsky, S. Peleg, and D. Avnir, *IEEE Trans. Pattern Anal. Machine Intell.*, 1995, **17**, 1154–1166; (b) H. Zabrodsky and D. Weinshall, *Comput. Vision Image Understanding*, 1997, **67**, 48–57; (c) H. Zabrodsky, 'Computational Aspects of Pattern Characterization – Continuous Symmetry', PhD Dissertation, Hebrew University, 1993.
19. I. Saragusti, I. Sharon, O. Katzenelson, and D. Avnir, *J. Archeol. Sci.*, 1998, in press.